Complexes Containing *cis*-$[Mo^{V}O_2]^+$ and *cis*-$[Mo^{V}O(OH)]^{2+}$ Centers

Zhiguang Xiao,* Robert W. Gable, Anthony G. Wedd, and Charles G. Young*

Contribution from the School of Chemistry, University of Melbourne, Parkville, Victoria 3052, Australia

Received July 27, 1995[⊗]

Abstract: Cobaltocene reduction of $LMo^{VI}O_2(SPh)$ complexes yielded extremely dioxygen-sensitive cobaltocenium salts of the *cis*-dioxo-Mo(V) radical anions *cis*-$[LMo^{V}O_2(SPh)]^-$, while sodium acenaphthalenide reduction of L^a-$Mo^{VI}O_2(SPh)$ yielded a complex sodium salt containing $[L^aMo^{V}O_2(SPh)]^-$ [L = hydrotris(3,5-dimethylpyrazol-1-yl)borate (L^a), hydrotris(3-isopropylpyrazol-1-yl)borate (L^b), or hydrotris(3,5-dimethyl-1,2,4-triazol-1-yl)borate (L^c)]. Crystals of $[CoCp_2][L^cMo^{V}O_2(SPh)]$·toluene were orthorhombic, space group *Pbca*, with $a = 17.695(3)$ Å, $b = 19.490(3)$ Å, $c = 21.925(4)$ Å, $V = 7561(2)$ Å^3 for $Z = 8$. The structure, refined using a full-matrix least-squares procedure and 2269 data, converged with $R = 0.067$ ($R_w = 0.067$). In the distorted octahedral anion, the metrical parameters of the *cis*-$Mo^{V}O_2$ fragment [Mo−O = 1.742(9) Å, O−Mo−O = 112.1(4)°] are significantly larger than those of $L^cMo^{VI}O_2(SPh)$ [average Mo−O = 1.700(6) Å, O−Mo−O = 103.9(2)°]. ^{18}O-Substitution of $[CoCp_2][L^{a,b}$-$Mo^{V}O_2(SPh)]$ permitted the assignment of bands at ca. 870 and 770 cm^{-1} to the ν_s and ν_{as} modes, respectively, of the *cis*-$Mo^{V}O_2$ fragment. Freshly prepared solutions of $[CoCp_2][LMo^{V}O_2(SPh)]$ exhibited a broad EPR signal (g, 1.92; $W_{1/2}$, 20 G) characteristic of a *cis*-$[Mo^{V}O_2]^+$ complex. The signal was stable when L = L^c but when L = L^a or L^b it was replaced by a proton-coupled signal characteristic of a *cis*-$[Mo^{V}O(OH)]^{2+}$ center. The complex L^a-$Mo^{V}O(OH)(SPh)$ was isolated as a coprecipitate with its conjugate base salt $[CoCp_2][L^aMo^{V}O_2(SPh)]$. It was characterized by infrared bands at 915 and 535 cm^{-1}, assigned to ν(Mo═O) and ν(Mo−OH) modes, respectively. The anions were readily converted to air-stable $LMo^{V}O(OSiMe_3)(SPh)$ upon reaction with Me_3SiCl and reacted with dioxygen to regenerate $LMo^{VI}O_2(SPh)$. The paper reports the first isolation in substance of compounds containing novel *cis*-$[Mo^{V}O_2]^+$ and *cis*-$[Mo^{V}O(OH)]^{2+}$ centers and the first crystallographic characterization of a *cis*-dioxo-Mo(V) species.

Introduction

In dioxo complexes of d^0 transition metals, favorable $p_\pi-d_\pi$ orbital interactions between the π-base oxo ligands and π-acid metal centers are optimized when a *cis* geometry is adopted; accordingly, all such complexes exhibit *cis* geometries.[1,2] However, upon one- or two-electron reduction, *cis*-$[MO_2]^{x+}$ complexes appear to be thermodynamically unstable with respect to isomerization to their *trans* forms, which can accommodate the extra electrons in nonbonding orbitals, or to decomposition.[1,2] To our knowledge, no detailed account of the isolation of any d^1 *cis*-$[MO_2]^{x+}$ coordination complex has appeared. Isolable d^2 *cis*-$[MO_2]^{x+}$ complexes are restricted to the elements rhenium,[3−5] ruthenium,[6−8] and osmium.[9−12] Many of the isolated Ru and Os complexes, as well as a number of *in situ* generated d^2 *cis*-dioxo-Ru and -Os complexes, are implicated in novel stoichiometric and catalytic oxygen atom transfer systems.[13]

The *cis*-$[Mo^{VI}O_2]^{2+}$ center dominates the chemistry of d^0 Mo(VI) complexes[14] and participates in many oxygen atom transfer reactions.[15−17] With few exceptions, one-electron reduction

[⊗] Abstract published in *Advance ACS Abstracts,* February 1, 1996.

(1) Nugent, W. A.; Mayer, J. M. *Metal-Ligand Multiple Bonds*, Wiley: New York, 1988.

(2) Theoretical treatments of bonding in MO_x fragments include the following: (a) Griffith, W. P. *Coord. Chem. Rev.* **1970**, *5*, 459. (b) Mingos, D. M. P. *J. Organomet. Chem.* **1979**, *179*, C29. (c) Tatsumi, K.; Hoffmann, R. *Inorg. Chem.* **1980**, *19*, 2656. (d) Rappe, A. K.; Goddard, W. A., III. *J. Am. Chem. Soc.* **1982**, *104*, 448. (e) Rappe, A. K.; Goddard, W. A., III. *J. Am. Chem. Soc.* **1982**, *104*, 3287. (f) Brower, D. C.; Templeton, J. L.; Mingos, D. M. P. *J. Am. Chem. Soc.* **1987**, *109*, 5203. (g) Cundari, T. R.; Drago, R. S. *Inorg. Chem.* **1990**, *29*, 2303. (h) Peng, G.; Nichols, J.; McCullough, E. A., Jr.; Spence, J. T. *Inorg. Chem.* **1994**, *33*, 2857.

(3) *cis*-$ReO_2I(PPh_3)_2$: (a) Freni, M.; Giusto, D.; Romiti, P.; Minghetti, G. *Gazz. Chim. Ital.* **1969**, *99*, 286. (b) Ciani, G. F.; D'Alfonso, G.; Romiti, P. F.; Sironi, A.; Freni, M. *Inorg. Chim. Acta* **1983**, *72*, 29. (c) Sullivan, B. P.; Brewer, J. C.; Gray, H. B. *Inorg. Synth.* **1992**, *29*, 146. The O−Re−O bond angle of 138.7(6)° in this five-coordinate complex is nearly midway between O−M−O angles typical of *cis* (ca. 105°) and *trans* (180°) complexes.

(4) *cis*-$[ReO_2(bpy)(py)_2]^+$: (a) Ram, M. S.; Johnson, C. S.; Blackburn, R. L.; Hupp, J. T. *Inorg. Chem.* **1990**, *29*, 238. (b) Blackburn, R. L.; Jones, L. M.; Ram, M. S.; Sabat, M.; Hupp, J. T. *Inorg. Chem.* **1990**, *29*, 1791. (c) Ram, R. S.; Hupp, J. T. *Inorg. Chem.* **1991**, *30*, 130.

(5) Abbreviations used: Ac = acenaphthalene or its radical anion; bpy = 2,2′-bipyridine; Cp = η^5-cyclopentadienyl; L = hydrotris(3,5-dimethylpyrazol-1-yl)borate (L^a), hydrotris(3-isopropylpyrazol-1-yl)borate (L^b), or hydrotris(3,5-dimethyl-1,2,4-triazol-1-yl)borate (L^c); L-N_2S_2 = dianion of *N*,*N*′-dimethyl-*N*,*N*′-bis(2-mercaptophenyl)-1,2-diaminoethane; L-NS_2 = dianion of 2,6-bis(2,2-diphenyl-2-mercaptoethyl)pyridine; L-N_2O_2 = dianion of *N*,*N*′-bis(2-hydroxyphenyl)-*N*,*N*′-dimethyl-1,2-diaminoethane; Me_3tcn = *N*,*N*′,*N*″-trimethyl-1,4,7-triazacyclononane; py = pyridine; THF = tetrahydrofuran; EHMO = extended Hückel molecular orbital; INDO = intermediate-neglect-of-differential-overlap; HOMO = highest occupied molecular orbital; LUMO = lowest unoccupied molecular orbital.

(6) *cis*-$[RuO_2Cl_3]^-$: Perrier, S.; Kochi, J. K. *Inorg. Chem.* **1988**, *27*, 4165.

(7) *cis*-$[RuO_2(O_2CMe)Cl_2]^-$: (a) Griffith, W. P.; Jolliffe, J. M.; Ley, S. V.; Williams, D. J. *J. Chem. Soc., Chem. Commun.* **1990**, 1219. (b) Griffith, W. P.; Jolliffe, J. M. *J. Chem. Soc., Dalton Trans.* **1992**, 3483.

(8) *cis*-$[RuO_2(Me_3tcn)(O_2CCF_3)]^+$: Cheng, W.-C.; Yu, W.-Y.; Cheung, K.-K.; Che, C.-M. *J. Chem. Soc., Chem. Commun.* **1994**, 1063.

(9) *cis*-$[OsO_2(O_2CMe)_3]^-$: (a) Criegee, R.; Marchand, B.; Wannovius, H. *Liebigs Ann. Chem.* **1942**, *550*, 99. (b) Behling, T.; Capparelli, M. V.; Skapski, A. C.; Wilkinson, G. *Polyhedron* **1982**, *1*, 840.

(10) *cis*-$[OsO_2(O_2CMe)Cl_2]^-$: (a) Griffith, W. P.; Jolliffe, J. M. *J. Chem. Soc., Dalton Trans.* **1992**, 3483.

(11) OsO_2(diolate)(N-donor): Pearlstein, R. M.; Blackburn, B. K.; Davis, W. M.; Sharpless, K. B. *Angew. Chem., Int. Ed. Engl.* **1990**, *29*, 639.

(12) *cis*-$[OsO_2(bpy)_2]^{2+}$: (a) Dobson, J. C.; Takeuchi, K. J.; Pipes, D. W.; Geselowitz, D. A.; Meyer, T. J. *Inorg. Chem.* **1986**, *25*, 2357. (b) Dobson, J. C.; Meyer, T. J. *Inorg. Chem.* **1989**, *28*, 2013.

(13) Goldstein, A. S.; Beer, R. H.; Drago, R. S. *J. Am. Chem. Soc.* **1994**, *116*, 2424 and references therein.

0002-7863/96/1518-2912$12.00/0

leads to $[Mo^VO]^{3+}$ or $[Mo^V_2O_3]^{4+}$ species, rather than stable *cis*-$[Mo^VO_2]^+$ complexes. Elimination and/or condensation reactions, initiated by coupled electron−proton transfer reactions involving an oxo ligand in the reduced complex, account for the formation of these thermodynamically favored species.[15,16] Kinetically controlled syntheses, which exploit ligands capable of retarding elimination and the close approach of molybdenum centers, are required for the generation of long-lived *cis*-$[Mo^VO_2]^+$ complexes. Only a small number of *cis*-$[Mo^{VI}O_2]^{2+}$ complexes are known to undergo a reversible, one-electron reduction on the cyclic voltammetric time scale.[18−23] The reduction products, which can be chemically generated in many cases, are formulated as *cis*-$[Mo^VO_2]^+$ complexes on the basis of EPR studies. Some of these complexes protonate to form *cis*-$[Mo^VO(OH)]^{2+}$ species, but the coligands are effective in retarding further reactions.[20−25] These formulations are consistent with extensive multifrequency EPR studies of $[(L\text{-}N_2S_2)MoO_2]^-$ and $(L\text{-}N_2S_2)MoO(OH)$ complexes and their ^{95,97}Mo-, ^{98}Mo-, ^{1}H-, ^{2}H-, and ^{17}O-labeled analogues.[5,20,26,27] Possible geometries and electronic structures for these species were predicted recently using *ab initio* and INDO molecular orbital methods, and in most cases, the results were concordant with those obtained from solution EPR studies.[2h] None of these complexes have been isolated in substance, and no structural information is available.

Recently, we reported a wide range of $LMo^{VI}O_2X$ complexes, some of which exhibited a reversible, one-electron reduction on cyclic voltammetric time scales, producing *cis*-$[LMo^VO_2X]^-$ (X = ER, E = O, S; R = alkyl, phenyl) species characterized by highly anisotropic frozen glass EPR spectra with low $\langle g \rangle$ values.[5,23] Protonation led to *cis*-$[Mo^VO(OH)]^{2+}$ complexes characterized by doublet EPR spectra arising from proton superhyperfine coupling.[23] We report here the isolation of various salts of the *cis*-dioxo-Mo(V) radical anions $[LMo^VO_2(SPh)]^-$, along with details of their spectroscopic, crystallographic, and electrochemical characterization. Aspects of this work have been communicated.[28,29] We also report evidence for the isolation of the conjugate acid of $[L^aMo^VO_2(SPh)]^-$, i.e., $L^aMo^VO(OH)(SPh)$. *cis*-$[Mo^VO(OH)]^{2+}$ centers have been implicated in the turnover of the enzymes sulfite oxidase and nitrate reductase;[15,16,30−33] this work represents the first isolation in substance of such a species. Kinetically controlled syntheses and the judicious choice of coligands for the *cis*-$[Mo^VO_2]^+$ center were crucial factors in the isolation and characterization of these extremely dioxygen-sensitive species.

Experimental Section

Materials and Methods. Complexes $LMo^{VI}O_2(SPh)$ were prepared as described previously.[22,23] Cobaltocene ($CoCp_2$) was prepared by literature methods[34] and purified by careful and repeated sublimation. Chlorotrimethylsilane was dried and distilled from $AlCl_3/CaH_2$. Acenaphthalene (Aldrich) was purified by chromatography on silica gel with dichloromethane as solvent, recrystallized from dichloromethane/methanol, and dried at 40−50 °C under vacuum. Flame-dried glassware, dinitrogen atmospheres, and carefully dried and deoxygenated solvents[35] were employed in all syntheses and manipulations in solution. The solvents employed for ^{18}O isotope studies were rigorously dried anaerobically by stirring over activated alumina immediately prior to use. The 95 atom % $H_2{}^{18}O$ was purchased from Aldrich Chemicals.

Infrared spectra were recorded on a Bio-Rad FTS-60A Fourier Transform IR spectrophotometer calibrated with polystyrene; complexes were sampled via dispersion in pressed KBr discs or via Nujol mulls between KBr plates. Air-sensitive samples were prepared in a glovebox and maintained under an inert atmosphere until the spectrum was recorded. EPR spectra were obtained on a Bruker ECS 106 EPR spectrometer using 1,1-diphenyl-2-picrylhydrazyl as reference; frozen solutions of $[CoCp_2][LMo^VO_2(SPh)]$ were prepared by dissolving the complex in an EPR tube under anaerobic conditions and immediately freezing the solution. Samples were melted and warmed to room temperature just before recording the liquid solution EPR spectrum. Near-IR and UV−visible spectra were recorded on Cary 17 and Hitachi 150-20 instruments, respectively. Electrochemical experiments were performed as described previously.[23] Acetonitrile solutions of the compounds (1−2 mM) in 0.2 M $Bu^n{}_4NBF_4$ were routinely employed. Potentials are quoted relative to the saturated calomel electrode (SCE). Electron impact (70 eV) mass spectrometric measurements were performed on a VG Micromass 7070 F mass spectrometer. Microanalyses were performed by the Analytische Laboratorien, Engelskirchen, Germany, or Atlantic Microlabs, Norcross, GA.

EHMO calculations were performed on a CAChe Tektronics system. The crystallographic coordinates of $L^aMo^{VI}O_2(SPh)$[23] and $[L^cMo^VO_2(SPh)]^-$ were used to build molecular structures for $[L^aMoO_2(SPh)]^{0/-}$ and $[L^cMoO_2(SPh)]^{0/-}$ complexes, with O−Mo−O angles of 102.6° and 112.1°, respectively. These complexes approximate C_s symmetry which is assumed in the orbital and EPR treatments presented in this paper. EHMO calculations on $[L^cMoO_2(SPh)]^{0/-}$ based on the coordinates of $L^cMoO_2(SPh)$[23] are not valid within these treatments due to the reduced (C_1) symmetry of this species in the solid state.[36] The presence of different L ligands had only a small effect on the outcome of the calculations, with the energies of the orbitals in the complexes of the electron-withdrawing L^c ligand being lower than those of the L^a complexes.

(14) Stiefel, E. I. In *Comprehensive Coordination Chemistry*; Wilkinson, G., Gillard, R. D., McCleverty, J. A., Eds.; Pergamon: Oxford, 1987; Chapter 36.5, p 1375.
(15) Young, C. G.; Wedd, A. G. In *Encyclopedia of Inorganic Chemistry*; King, R. B., Ed.; Wiley: New York, 1994; p 2330 and references therein.
(16) Enemark, J. H.; Young, C. G. *Adv. Inorg. Chem.* **1993**, *40*, 1 and references therein.
(17) (a) Sheldon, R. A.; Kochi, J. K. *Metal-Catalysed Oxidations of Organic Compounds*; Academic: New York, 1981. (b) Holm, R. H. *Chem. Rev.* **1987**, *87*, 1401.
(18) Pickett, C.; Kumar, S.; Vella, P. A.; Zubieta, J. *Inorg. Chem.* **1982**, *21*, 908.
(19) Kaul, B. B.; Enemark, J. H.; Merbs, S. L.; Spence, J. T. *J. Am. Chem. Soc.* **1985**, *107*, 2885.
(20) Dowerah, D.; Spence, J. T.; Singh, R.; Wedd, A. G.; Wilson, G. L.; Farchione, F.; Enemark, J. H.; Kristofzski, J.; Bruck, M. *J. Am. Chem. Soc.* **1987**, *109*, 5655.
(21) Farchione, F.; Hanson, G. R.; Rodrigues, C. G.; Bailey, T. D.; Bagchi, R. N.; Bond, A. M.; Pilbrow, J. R.; Wedd, A. G. *J. Am. Chem. Soc.* **1986**, *108*, 831.
(22) Roberts, S. A.; Young, C. G.; Kipke, C. A.; Cleland, W. E., Jr.; Yamanouchi, K.; Carducci, M. D.; Enemark, J. H. *Inorg. Chem.* **1990**, *29*, 3650.
(23) Xiao, Z.; Bruck, M. A.; Doyle, C.; Enemark, J. H.; Grittini, C.; Gable, R. W.; Wedd, A. G.; Young, C. G. *Inorg. Chem.* **1995**, *34*, 5950.
(24) Subramanian, P.; Kaul, B.; Spence, J. T. *J. Mol. Catal.* **1984**, *23*, 163.
(25) Hinshaw C. J.; Spence, J. T. *Inorg. Chim. Acta* **1986**, *125*, L17.
(26) Wilson, G. L.; Greenwood, R. J.; Pilbrow, J. R.; Spence, J. T.; Wedd, A. G. *J. Am. Chem. Soc.* **1991**, *113*, 6803.
(27) Greenwood, R. J.; Wilson, G. L.; Pilbrow, J. R.; Wedd, A. G. *J. Am. Chem. Soc.* **1993**, *115*, 5385.
(28) Xiao, Z.; Young, C. G.; Enemark, J. H.; Wedd, A. G. *J. Am. Chem. Soc.* **1992**, *114*, 9194.
(29) Xiao, Z.; Gable, R. W.; Wedd, A. G.; Young, C. G. *J. Chem. Soc., Chem. Commun.* **1994**, 1295.
(30) *Molybdenum Enzymes, Cofactors and Model Systems*, Stiefel, E. I., Coucouvanis, D., Newton, W. E., Eds.; ACS Symposium Series 535; American Chemical Society: Washington, DC, 1993.
(31) Young, C. G.; Wedd, A. G., in ref 30, p 70.
(32) Bray, R. C. *Adv. Enz. Rel. Areas Mol. Biol.* **1980**, *51*, 107.
(33) Bray, R. C. *Q. Rev. Biophys.* **1988**, *21*, 299.
(34) (a) Wilkinson, G.; Cotton, F. A.; Birmingham, J. M. *J. Inorg. Nucl. Chem.* **1956**, *2*, 95. (b) King, R. B. *Organometallic Syntheses*; Academic: New York, 1965; Vol. 1, p 70.
(35) Perrin, D. D.; Armarego, W. L. F.; Perrin, D. R. *Purification of Laboratory Chemicals*, 2nd ed.; Pergamon Press: Oxford, 1980.
(36) The C_1 symmetry of $L^cMo^{VI}O_2(SPh)$ is a consequence of the significant twisting of the SPh^- ligand out of the mirror plane. Interestingly, the orientation of the potentially π-donor SPh^- ligand impacts on the symmetry and energy of the π-manifold of the MoO_2 fragment. This effect was, however, not examined in detail.

Syntheses. [$CoCp_2$][$L^aMo^VO_2$(SPh)]. A solution of $CoCp_2$ (0.14 g, 0.74 mmol) in acetonitrile (10 mL) was filtered onto $L^aMo^{VI}O_2$(SPh) (0.20 g, 0.37 mmol), and the mixture was stirred for 15 min. The resultant green microcrystals were filtered, washed three times with acetonitrile, and then dried under vacuum. Yield 0.19 g (70%). Anal. Calcd for $C_{31}H_{37}BCoMoN_6O_2S$: C, 51.47; H, 5.16; N, 11.62; S, 4.43. Found: C, 51.23; H, 5.28; N, 11.90; S, 4.33. Electrochemistry (CH_3CN): $E_{1/2}(Mo^{VI}/Mo^V) = -0.76$ V. ^{18}O-Enriched [$CoCp_2$][$L^aMo^VO_2$(SPh)] was prepared similarly using enriched $L^aMo^{VI}O_2$(SPh) prepared as described below. The level of ^{18}O in [$CoCp_2$][$L^aMo^VO_2$(SPh)] was found to be the same as that in the starting complex $L^aMo^{VI}O_2$(SPh) by mass spectrometric analysis of $L^aMo^VO(OSiMe_3)$(SPh) produced from the salt upon reaction with Me_3SiCl (vide infra).

$L^aMo^{VI}O_2$(SPh) (80 Atom % ^{18}O). A mixture of $L^aMo^{VI}O_2$(SPh) (0.40 g, 0.75 mmol) and PPh_3 (0.090 g, 0.34 mmol) was treated with alumina-dried tetrahydrofuran (10 mL) and $H_2{}^{18}O$ (250 mg, 12.5 mmol). The dark brown mixture was stirred at room temperature under dinitrogen for 7 h during which the solution slowly turned dark green. Dioxygen was then bubbled through the solution to regenerate the initial brown color. The solution was immediately evaporated to dryness under vacuum and chromatographed on silica gel in air using toluene as eluent. The dark brown fraction was collected, and the complex was recrystallized from dichloromethane/methanol. Yield 0.29 g (72%). The isotope-independent properties of this substance were identical to those of an authentic sample of $L^aMo^{VI}O_2$(SPh).[22,23] Infrared data were consistent with the presence of $^{16}O^{16}O$, $^{16}O^{18}O$, and $^{18}O^{18}O$ isotopomers. Mass spectra of the $L^aMo^VO(OSiMe_3)$(SPh) derivative confirmed enrichment in ^{18}O to the 80 atom % level: for $[L^aMoO(OSiMe_3)]^+$ *m/z* (%) 494 (4), 495 (7), 496 (22), 497 (23), 498 (61), 499 (50), 500 (74), 501 (87), 502 (100), 503 (69), 504 (85), 505 (29), 506 (30), 507 (8).

[$CoCp_2$][$L^bMo^VO_2$(SPh)]. A solution of $CoCp_2$ (0.14 g, 0.74 mmol) in toluene (10 mL) was filtered onto a stirred solution of $L^bMo^{VI}O_2$(SPh) (0.20 g, 0.34 mmol) in toluene (10 mL). Green microcrystals were filtered off, washed three times with toluene, and dried in vacuum. Yield 0.18 g (69%). Anal. Calcd for $C_{34}H_{43}BCoMoN_6O_2S$: C, 53.35; H, 5.66; N, 10.98. Found: C, 53.10; H, 5.70; N, 10.84. Electrochemistry (CH_3CN): $E_{1/2}(Mo^{VI}/Mo^V) = -0.65$ V. ^{18}O-Enriched $L^bMo^{VI}O_2$(SPh) and [$CoCp_2$][$L^bMo^VO_2$(SPh)] were prepared by the methods described for the L^a analogues.

[$CoCp_2$][$L^cMo^VO_2$(SPh)]. Method 1. A solution of $CoCp_2$ (0.19 g, 1.0 mmol) in *n*-hexane (15 mL) was filtered into a Schlenk flask containing $L^cMo^{VI}O_2$(SPh) (0.30 g, 0.56 mmol) and a magnetic stirring bar. Dropwise addition of dichloromethane (5 mL) to the stirred suspension produced the pale green product, which was filtered, washed three times with *n*-hexane, and dried under vacuum. Yield, 0.35 g (86%).

Method 2. A solution of $CoCp_2$ (0.09 g, 0.47 mmol) in toluene (5 mL) was added dropwise to a stirred solution of $L^cMo^{VI}O_2$(SPh) (0.14 g, 0.26 mmol) in toluene (5 mL). The resultant green precipitate was filtered, washed with toluene, and dried under vacuum. Yield 0.17 g (90%). Anal. Calcd for $C_{28}H_{34}BCoMoN_9O_2S$: C, 46.30; H, 4.72; N, 17.35. Found: C, 46.03; H, 4.65; N, 17.11. Electronic spectrum (CH_2Cl_2): 330 (sh, ~3000), 420 (sh, ~1000), 780 (40), 1110 nm (ϵ 30 M^{-1} cm^{-1}). Electrochemistry (CH_3CN): $E_{1/2}(Mo^{VI}/Mo^V) = -0.53$ V.

[$Na(thf)_2$][$L^aMo^VO_2$(SPh)]·*x*NaX (X = Cl and/or OH). Tetrahydrofuran (20 mL) was added to a mixture of acenaphthalene (0.22 g, 1.4 mmol) and freshly cut sodium metal (0.17 g, 7.4 mmol) and the solution stirred at room temperature overnight. Unreacted Na metal was removed and the solution added to PPh_4Cl (0.60 g, 1.6 mmol). The mixture was stirred at room temperature for 1 h before being filtered into a Schlenk flask containing $L^aMo^{VI}O_2$(SPh) (0.60 g, 1.2 mmol). A yellow-green solid formed upon stirring. It was collected by filtration, washed with tetrahydrofuran (3 × 5 mL), and dried under vacuum. Yield 0.30−0.50 g (48−80%). Microanalysis. Sample 1. $x = 2.2$ (X = Cl). Calcd for $C_{29}H_{43}BCl_{2.2}MoN_6Na_{3.2}O_4S$: C, 42.00; H, 5.17; N, 10.13; S, 3.63. Found: C, 41.97; H, 5.22; N, 10.13; S, 3.86. Sample 2. $x = 1.6$ (X = Cl). Calcd for $C_{29}H_{43}BCl_{1.6}MoN_6Na_{2.6}O_4S$: C, 43.81; H, 5.45; N, 10.57; S, 4.03; Cl, 7.13. Found: C, 43.81; H, 5.44; N, 10.80; S, 3.93, Cl, 5.82. Infrared spectra (Nujol mull) were identical for samples 1 and 2: ν(B−H) 2512 m, $\nu(Mo^VO_2)$ 853 m, 777 vs cm^{-1}.

"L^aMo^VO(OH)(SPh)". A solution of $CoCp_2$ (0.14 g, 0.74 mmol) in acetonitrile (10 mL) was added to a solution of $L^aMo^{VI}O_2$(SPh) (0.20 g, 0.37 mmol) in dichloromethane (5 mL). After stirring at room temperature for 2 h, the volume was reduced to *ca.* 10 mL under reduced pressure. The green microcrystals were filtered, washed with acetonitrile, and dried under vacuum. Yield 0.08 g. An ^{18}O-labeled sample was prepared similarily using $L^aMo^{VI}O_2$(SPh) (55 atom % ^{18}O).

$L^aMo^VO(OSiMe_3)$(SPh). A freshly deoxygenated solution of Me_3SiCl (0.5 mL) in acetonitrile (15 mL) was added to [$CoCp_2$][$L^aMo^VO_2$(SPh)] (0.40 g, 0.55 mmol). The mixture turned dark green immediately. After stirring for 10 min, the solution was evaporated to dryness and the residue chromatographed in air on silica using 2:1 *n*-pentane: dichloromethane as eluent. The first dark green band was collected and a dark green solid isolated by addition of methanol. Yield, 0.31 g (92%). Anal. Calcd for $C_{24}H_{36}BMoN_6O_2SSi$: C, 47.45; H, 5.97; N, 13.83; S, 5.28. Found: C, 47.57; H, 5.69; N, 13.88; S, 5.20. Mass spectrum (*m/z*): 609. EPR (toluene): *g*, 1.942, $A(^{95,97}Mo)$, 44.0 × 10^{-4} cm^{-1}. Infrared (KBr): ν(B−H) 2549 m, ν(Si−C) 1249 m, ν(Mo=O) 953 s, ν(Si−O) 920 s, br cm^{-1}. Electrochemistry (CH_3CN): Mo^V/Mo^{IV} −0.89 (reversible) and Mo^{VI}/Mo^V +0.63 V (irreversible). ^{18}O-Enriched $L^aMo^VO(OSiMe_3)$(SPh) was prepared similarly using [$CoCp_2$][$L^aMo^VO_2$(SPh)] (80 atom % ^{18}O). Infrared (KBr): ν(B−H) 2548 m, ν(Si−C) 1249 m, $\nu(Mo=^{18}O)$ 910 s, $\nu(Si-^{18}O)$ 875 s, br cm^{-1}.

The minor product isolated from the second bright green band was identified as L^aMo^VOCl(SPh).[37]

$L^aMo^VO(OSiMe_3)$(SPh) was prepared similarly from the salts [$Na(thf)_2$][$L^aMo^VO_2$(SPh)]·*x*NaX (X = Cl and/or OH) in ca. 64% yield.

$L^bMo^VO(OSiMe_3)$(SPh). The synthesis was similar to the L^a complex using [$CoCp_2$][$L^bMo^VO_2$(SPh)] as starting material. The product was purified by chromatography in air on silica using 2:1 *n*-pentane:dichloromethane as eluent. Yield 80%. Mass spectrum (*m/z*): 651. EPR (toluene): *g*, 1.943, $A(^{95,97}Mo)$, 44.2 × 10^{-4} cm^{-1}. Infrared (KBr): ν(B−H) 2488m, ν(Si−C) 1247m, ν(Mo=O) 956s, ν(Si−O) 915 s, br cm^{-1}. Cyclic voltammetry (CH_3CN): Mo^V/Mo^{IV} −0.79 (reversible) and Mo^{VI}/Mo^V +0.73 V (irreversible).

$L^cMo^VO(OSiMe_3)$(SPh). An analogous synthesis using [$CoCp_2$][$L^cMo^VO_2$(SPh)] as starting material produced the desired complex as major product, as demonstrated by thin layer chromatography of the initial product mixture. The complex is unstable in solution, and significant decomposition occurred during chromatographic workup on a silica column with acetonitrile as eluent. EPR (toluene): *g*, 1.944, $A(^{95,97}Mo)$, 44.0 × 10^{-4} cm^{-1}. Infrared (KBr): ν(B−H) 2526m, ν(Si−C) 1243m, ν(Mo=O) 956s, ν(Si−O) 907s, br cm^{-1}.

Crystallography. Dark green crystals of [$CoCp_2$][$L^cMo^VO_2$(SPh)]·toluene were obtained by dissolution *in situ* of the precipitate in synthetic method 2 by the addition of a minimum quantity of acetonitrile, followed by cooling of the solution at −20 °C for 3 days. A plate of approximate dimensions 0.40 × 0.38 × 0.06 mm was sealed in a Lindemann glass capillary tube under a dinitrogen atmosphere. Accurate values of the unit cell parameters and crystal orientation were obtained by a least-squares procedure from the angular settings of 25 carefully centered reflections. Intensity data were collected using an Enraf-Nonius CAD-4MachS single-crystal X-ray diffractometer using the ω:2θ scan method, with Mo Kα radiation (graphite crystal monochromator) $\lambda = 0.71069$ Å, at 294(1) K. Although protected from the atmosphere, the crystal decomposed significantly on exposure to the X-ray beam; three intensity control reflections, monitored every 9600 s of X-ray exposure time, showed a 35% deterioration in intensity. The data were corrected in accordance with this variation, as well as for Lorentz and polarization effects, but not for extinction. Analytical absorption corrections were applied, the maximum and minimum transmission factors being 0.951 and 0.756, respectively. Crystallographic data are summarized in Table 1.

The structure was solved using a combination of Patterson map, direct methods, and difference syntheses.[38] The positions of few

(37) Cleland, W. E., Jr.; Barnhart, K. M.; Yamanouchi, K.; Collison, D.; Mabbs, F. E.; Ortega, R. B.; Enemark, J. H. *Inorg. Chem.* **1987**, *26*, 1017.

(38) (a) Sheldrick, G. M. SHELXS86, Program for Crystal Structure Solution, *Acta Cryst*. **1990**, *A46*, 467. (b) Sheldrick, G. M. SHELX76, Program for Crystal Structure Determination; Cambridge University: England, 1976.

Table 1. Crystallographic Data for $[CoCp_2][L^cMo^VO_2(SPh)]$·toluene

formula	$C_{35}H_{42}BCoMoN_9O_2S$
color	dark green
fw	818.5
crystal system	orthorhombic
space group	*Pbca* (No. 61)
a, Å	17.695(3)
b, Å	19.490(3)
c, Å	21.925(4)
V, Å^3	7561(2)
Z	8
ρ_{calcd}, g/cm^3	1.438
radiation (λ), Å	Mo Kα (0.71069)
μ, cm^{-1}	8.35
transmission factors, max	0.951
min	0.756
2θ limits	$4.4 \le 2\theta \le 50°$
data collected	h,k,l
no. of data collected	8677
no. of unique data	6617
R_{int}	0.019
no. of data used in refinement	2269 [$I \ge 2.5\sigma(I)$]
final R^a	0.067
final $R_w{}^b$	0.067

^{a} $R = \sum(|F_o| - |F_c|)/\sum(F_o)$. ^{b} $R_w = [\sum w(|F_o| - |F_c|)^2/\sum wF_o^2]^{1/2}$.

Table 2. Bond Distances and Angles for the Anion in $[CoCp_2][L^cMo^VO_2(SPh)]$·toluene

Distances (Å)					
Mo−O(1)	1.742(9)	Mo−O(2)	1.742(9)	Mo−S	2.442(4)
Mo−N(11)	2.277(11)	Mo−N(21)	2.410(12)	Mo−N(31)	2.334(10)
S−C(1)	1.811(15)				

Angles (deg)			
O(1)−Mo−O(2)	112.1(4)	O(1)−Mo−S	96.3(4)
O(2)−Mo−S	95.5(4)	O(1)−Mo−N(11)	90.1(5)
O(1)−Mo−N(21)	84.3(5)	O(1)−Mo−N(31)	157.7(5)
O(2)−Mo−N(11)	90.4(5)	O(2)−Mo−N(21)	161.6(5)
O(2)−Mo−N(31)	87.5(5)	S−Mo−N(11)	168.9(4)
S−Mo−N(21)	90.7(4)	S−Mo−N(31)	91.9(4)
N(11)−Mo−N(21)	80.9(6)	N(11)−Mo−N(31)	78.9(5)
N(21)−Mo−N(31)	75.0(5)	Mo−S−C(1)	110.5(6)

hydrogens could be found in the difference maps, and subsequently none were included in the model. Full-matrix least-squares refinement, with anisotropic temperature factors applied to each of the non-hydrogen atoms, and using a weighting scheme of type $k[\sigma^2(F) + gF^2]^{-1}$, converged with R 0.067, R_w 0.067, k 2.699, and g 0.00047. The maximum peak heights in the final difference map were 0.68 e Å^{-3}, close to the Mo atom, and 0.48 e Å^{-3} surrounding the toluene molecule, indicating slight disorder for this molecule. An analysis of variance showed no unusual features.

The atomic scattering factors employed for non-metal atoms were those incorporated in the SHELX76 program.[38b] Coefficients for the scattering curves for atomic Co and Mo were obtained from ref 39; corrections were made for anomalous dispersion. Calculations were carried out on a Microvax II 630QB computer. Fractional atomic coordinates are available as supporting information. The structure and numbering scheme are represented using ORTEP.[40] Selected bond distances and angles are given in Table 2.

Results

Cobaltocenium Salts of $[LMo^VO_2(SPh)]^-$. The $[CoCp_2]^+/CoCp_2$ couple occurs at $E_{1/2} = -0.94$ V vs SCE in acetonitrile and so cobaltocene is thermodynamically capable of reducing $LMo^{VI}O_2(SPh)$ [$E_{1/2} = -0.76$ (L^a), -0.65 (L^b), -0.53 (L^c) V].[23] Excess cobaltocene and precipitation of the product from acetonitrile ensured completion of the reaction for L = L^a:

$$L^aMo^{VI}O_2(SPh) + CoCp_2 \rightarrow [CoCp_2][L^aMo^VO_2(SPh)] \quad (1)$$

The equivalent salts for ligands L^b and L^c required toluene or alkanes as solvents as they were soluble in acetonitrile. All three salts were extremely sensitive to oxidation by dioxygen.

Cyclic voltammograms of each salt at a glassy carbon electrode in acetonitrile revealed three reversible waves assignable to Mo^{VI}/Mo^V, $[CoCp_2]^+/CoCp_2$, and $CoCp_2/[CoCp_2]^-$ couples;[22,23,41] the cyclic voltammogram of $[CoCp_2][L^aMo^VO_2(SPh)]$ is shown in Figure 1. Addition of $LMo^{VI}O_2(SPh)$ increases the peak current of the first couple while addition of $CoCp_2$ increases the peak current of the latter two. The lower magnitude of the peak current of the first couple relative to the other two is consistent with lower diffusion coefficients for the molybdenum complexes relative to $CoCp_2$.

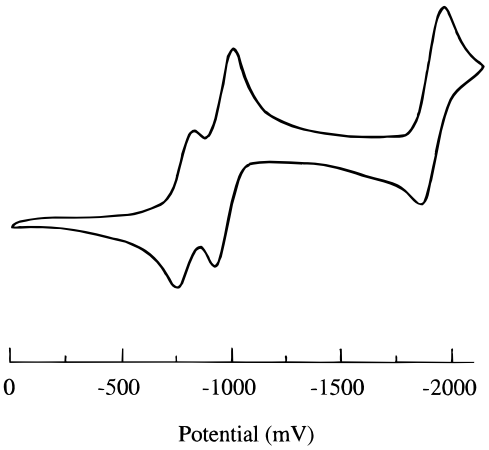

Figure 1. Cyclic voltammogram of $[CoCp_2][L^aMo^VO_2(SPh)]$ in CH_3CN. Conditions: glassy carbon electrode; scan rate = 100 mV/s; 0.2 M $Bu^n{}_4NBF_4$; vs SCE.

EPR data are summarized in Table 3. A freshly prepared solution of $[CoCp_2][L^aMo^VO_2(SPh)]$ in carefully dried dichloromethane exhibited a very broad EPR signal at $g = 1.920$ (Figure 2a). This signal was identical to that generated by reaction of $L^aMo^{VI}O_2(SPh)$ with excess $Bu^n{}_4NSH$ in THF and the initial signal observed upon electrochemical reduction of $L^aMo^{VI}O_2(SPh)$ in dry THF at room temperature;[23] it is assigned to the anionic species $[L^aMo^VO_2(SPh)]^-$. However, at room temperature, the spectrum converted rapidly to a proton-coupled EPR signal ($g = 1.953$, $A(^{95,97}Mo) = 43.2 \times 10^{-4}$ cm^{-1}, $A(^1H) = 13.1 \times 10^{-4}$ cm^{-1}) (Figure 2b), identical to that generated by electrochemical reduction of $L^aMo^{VI}O_2(SPh)$ in wet solvent.[23] This signal is assigned to $L^aMo^VO(OH)(SPh)$. When the solution was frozen, the highly anisotropic EPR signal characteristic of $[L^aMo^VO_2(SPh)]^-$ [23] was observed (Figure 2c). The signal assigned to $L^aMo^VO(OH)(SPh)$ was observed when the glass was allowed again to thaw to room temperature. These observations indicate the presence of an equilibrium between $[L^aMo^VO_2(SPh)]^-$ and $L^aMo^VO(OH)(SPh)$ in solution:

$$[L^aMo^VO_2(SPh)]^- + H_2O \rightleftharpoons L^aMo^VO(OH)(SPh) + OH^- \quad (2)$$

The position of the equilibrium appears to be phase and/or temperature dependent. Similar behavior was observed in the case of $[CoCp_2][L^bMo^VO_2(SPh)]$. However, dissolution of $[CoCp_2][L^cMo^VO_2(SPh)]$ in dichloromethane under the same conditions produced a clean EPR spectrum assignable to the

(39) *International Tables for X-Ray Crystallography*; Kluwer: Dordrecht; 1993, (a) Vol. C, p 500, (b) Vol. C, p 219.
(40) Johnson, C. K. ORTEPII. Report ORNL-5138; Oak Ridge National Laboratory: Oak Ridge, TN, 1976.
(41) (a) Geiger, W. E., Jr. *J. Am. Chem. Soc.* **1974**, *96*, 2632. (b) Koelle, U. *J. Organomet. Chem.* **1978**, *152*, 225.

Table 3. EPR Data of $[LMo^{V}O_2(SPh)]^-$ in Dichloromethane[a]

L	g_1 (g_{zz})[c]	g_2 (g_{yy})[c]	g_3 (g_{xx})[c]	A_1 (A_{zz})[c]	A_2[b] (A_{yy})[c]	A_3 (A_{xx})[c]	g	A	$W_{1/2}$ (G)
L^a	1.991	1.931	1.843	27.9	28.4	67.9	1.920	41.4	20
L^b	1.994	1.938	1.842	29.0	~26	~67	1.920	40.6	20
L^c	1.994	1.936	1.844	27.0	~25	~68	1.923	40.0	19
L-N_2S_2[d]	1.987	1.916	1.811	27.1	31.2	68.8	1.904	42.4	

[a] Anisotropic data obtained from frozen-glass samples at 77 K; isotropic data obtained from solutions at ambient temperatures. A ($\times 10^{-4}$ cm^{-1}) values estimated directly from spectra. [b] Values estimated from $3A - A_1 - A_3$. [c] Tentative assignments (see text). [d] From ref 26: complex implied is $[(L\text{-}N_2S_2)MoO_2]^-$.

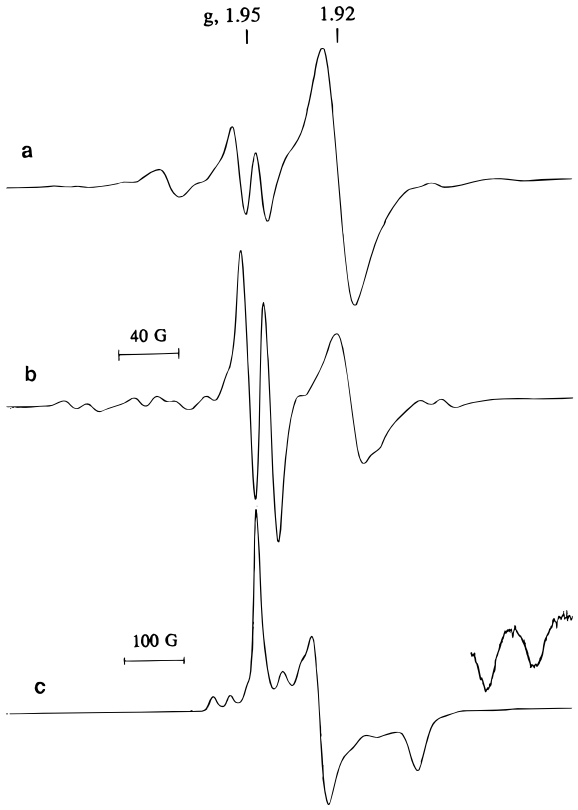

Figure 2. EPR spectra of $[CoCp_2][L^aMo^{V}O_2(SPh)]$ in CH_2Cl_2: (a) freshly prepared solution at 293 K; (b) after standing for *ca.* 20 min at 293 K [spectra (a) and (b) have the same scale]; (c) solution (b) at 77 K.

anion $[L^cMo^{V}O_2(SPh)]^-$. This ion was stable under all conditions and did not undergo protonation. The relative stability of $[L^cMo^{V}O_2(SPh)]^-$ permitted the growth of X-ray quality crystals of $[CoCp_2][L^cMo^{V}O_2(SPh)]$·toluene.

Infrared studies of ^{16}O- and ^{18}O-labeled $[CoCp_2][LMo^{V}O_2(SPh)]$ were undertaken to assist the assignment of the $\nu_s(MoO_2)$ and $\nu_{as}(MoO_2)$ vibration modes of the complex anions. Selected infrared spectral data are listed in Table 4. The theoretical treatments applied to the data are summarized in the Appendix. The spectrum of $[CoCp_2][L^aMo^{V}O_2(SPh)]$ exhibited bands characteristic of the L^a ligand (ν(BH) 2524 m cm^{-1}; ν(CN) 1542 s cm^{-1}) and the cobaltocenium cation (3098, 1414, 1008, 858, and 460 cm^{-1}).[42] Examination of the 1100−450 cm^{-1} region of the spectrum (Figure 3a) revealed the absence of a strong absorption typical of the $[Mo^{V}O]^{3+}$ unit between 1000 and 880 cm^{-1}. However, a sharp, strong band was observed at 767 cm^{-1}. When the sample was exposed to air, this band lost intensity and two absorptions typical of a *cis*-$[Mo^{VI}O_2]^{2+}$ center appeared at 922 and 890 cm^{-1} (Figures 3b and 3c). In 80 atom % ^{18}O-labeled $[CoCp_2][L^aMo^{V}O_2(SPh)]$, the 767 cm^{-1} band was virtually absent and two bands at 748 and 730 cm^{-1} were observed (Figure 4a); these are assigned to the $\nu_{as}(Mo^{V}O_2)$ modes of the $^{16}O^{18}O$ and $^{18}O^{18}O$ isotopomers, respectively. Although obscured by other bands, there was evidence of a $\nu_s(Mo^{V}O_2)$ band at *ca.* 865 cm^{-1} which shifted to 822 cm^{-1} in the $^{18}O^{18}O$ isotopomer (Figure 4a). The corresponding band for the $^{16}O^{18}O$ isotopomer was not observed presumably due to overlap with other absorptions.

(42) The infrared bands for $[CoCp_2]^+$ were identified by comparison with the infrared spectra of $[CoCp_2]Cl$ and $[CoCp_2]Br$.

Table 4. Infrared Assignments of $\nu_s(MoO_2)$ and $\nu_{as}(MoO_2)$ Modes (cm^{-1})[a]

	$^{16}O^{16}O$		$^{16}O^{18}O$		$^{18}O^{18}O$	
complex	ν_s	ν_{as}	ν_s	ν_{as}	ν_s	ν_{as}
$L^aMo^{VI}O_2(SPh)$	922 (923)	890	911	856	877	849 (848)
$L^bMo^{VI}O_2(SPh)$	927 (926)	899	916	863	880	855 (856)
$(L\text{-}NS_2)Mo^{VI}O_2$[b]	945 (945)	909	933	878	898	864 (867)
$[L^aMo^{V}O_2(SPh)]^-$ [c]	865(?) (865)	767		748	822	730 (731)
$[L^bMo^{V}O_2(SPh)]^-$ [c]	879 (879)	777	856		835	~743 (741)
$[L^cMo^{V}O_2(SPh)]^-$ [c]	876	776				

[a] The ν_s values calculated using $\nu_s^{18}/\nu_s^{16} = 0.950$ and ν_{as} using eq A1 are given in parentheses. The observed O−Mo−O angle (θ) for $L^aMo^{VI}O_2(SPh)$ and $[L^cMo^{V}O_2(SPh)]^-$ is used for $L^bMo^{VI}O_2(SPh)$ and $[L^{a,b}Mo^{V}O_2(SPh)]^-$, respectively. No labeling studies were possible for the L^c complex. [b] Reference 60. [c] Cobaltocenium salts.

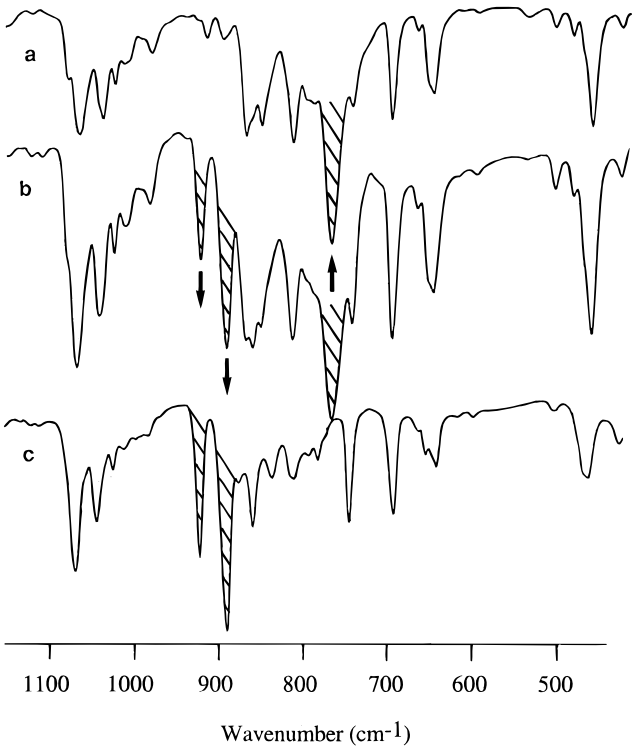

Figure 3. Infrared spectra of $[CoCp_2][L^aMo^{V}O_2(SPh)]$ (Nujol mull): (a) initial; (b) after standing in air for 6 min; (c) after standing in air for 30 min. Disappearance and in-growth of unobscured $\nu(MoO_2)$ bands are indicated by arrows.

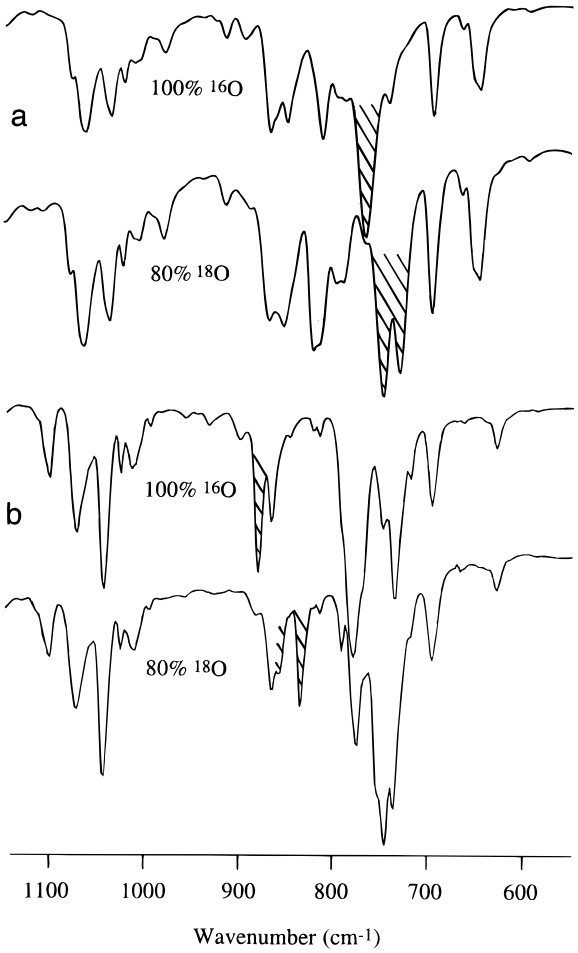

Figure 4. Infrared spectra of ^{16}O- and ^{18}O-substituted materials (Nujol mull): (a) $[CoCp_2][L^aMo^VO_2(SPh)]$; (b) $[CoCp_2][L^bMo^VO_2(SPh)]$. Unobscured $\nu(MoO_2)$ bands only are shaded.

The above assigments were supported by equivalent experiments involving $[CoCp_2][L^bMo^VO_2(SPh)]$. Bands assignable to the $\nu_s(MoO_2)$ absorptions of the $^{16}O^{16}O$, $^{16}O^{18}O$, and $^{18}O^{18}O$ isotopomers in 80 atom % ^{18}O-labeled compound are observed at 879, 856, and 835 cm^{-1}, respectively (Figure 4b), this time without interference from other bands. The $\nu_{as}(MoO_2)$ modes of the compound are obscured somewhat but the $^{16}O^{16}O$ and $^{18}O^{18}O$ components of $\nu_{as}(MoO_2)$ are estimated to occur close to 777 and 743 cm^{-1}, respectively. Attempts to synthesize ^{18}O forms of $L^cMo^{VI}O_2(SPh)$ were unsuccessful.

The X-ray crystal structure of $[CoCp_2][L^cMo^VO_2(SPh)]\cdot$toluene has been communicated;[29] details are summarized in Tables 1−2 and an ORTEP view of the anion is shown in Figure 5. We briefly reiterate the important features of this structure. The anion, in which molybdenum coordinates a facially tridentate triazolylborate ligand and mutually *cis* oxo and thiophenolate ligands, exhibits a distorted octahedral structure. The Mo atom is displaced from the midpoint of the equatorial plane defined by O(1), O(2), N(21), and N(31), toward the oxo ligands. The Mo−O(1) and Mo−O(2) bond distances are equal at 1.742 (9) Å, and the O(1)−Mo−O(2) angle is 112.1 (4)°. A noticeable *trans* influence is associated with the terminal oxo ligands. The Mo−S distance and Mo−S−C(1) angle are 2.442(4) Å and 110.5(6)°, respectively. The orientation of the phenyl group [Mo−S−C(1)−C(2) torsion angle −12.9(3)°] appears to be dictated primarily by the position of neighboring $[CoCp_2]^+$ counterions.

A Complex Sodium Salt. The preparation of $PPh_4[L^aMo^VO_2(SPh)]$ was attempted by reduction of $L^aMo^{VI}O_2(SPh)$ with sodium acenaphthalenide in the presence of PPh_4Cl in THF:

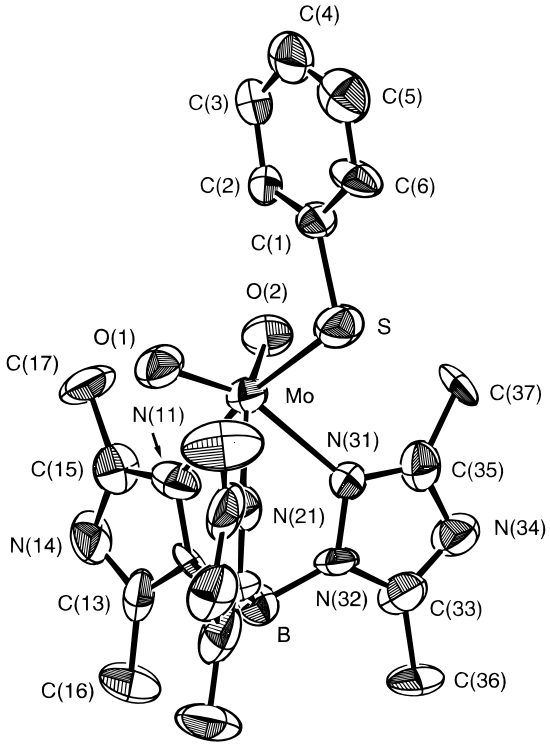

Figure 5. Structure of the anion in $[CoCp_2][L^cMo^VO_2(SPh)]\cdot$toluene. The numbering of the triazole ring containing N(21) parallels those shown for the other two rings.

$$NaAc + L^aMo^{VI}O_2(SPh) + PPh_4Cl_{(s)} \rightarrow PPh_4[L^aMo^VO_2(SPh)] + NaCl_{(s)} + Ac \quad (3)$$

As is evident from the following properties, the green product was not $PPh_4[L^aMo^VO_2(SPh)]$: (i) Infrared bands characteristic of PPh_4^+ were absent. Infrared bands at 853 and 777 cm^{-1} were assigned to the $\nu_s(MoO_2)$ and $\nu_{as}(MoO_2)$ modes of the $[L^aMo^VO_2(SPh)]^-$ anion; upon exposure to air, these bands disappeared and the equivalent absorptions of $L^aMo^{VI}O_2(SPh)$ grew in intensity. The compound was oxidized by air to $L^aMo^{VI}O_2(SPh)$. (ii) A single reversible couple at −0.76 V vs SCE was observed in the cyclic voltammogram in acetonitrile; it may be assigned to the $L^aMo^{VI}O_2(SPh)/[L^aMo^VO_2(SPh)]^-$ couple.[23] (iii) EPR spectra in dichloromethane were indistinguishable from those of $[CoCp_2][L^aMo^VO_2(SPh)]$ (Figure 2). (iv) Reaction with Me_3SiCl produced $L^aMo^VO(OSiMe_3)(SPh)$ in 64% isolated yield.

Sodium was detected qualitatively,[43] and microanalytical data were consistent with the presence of $[Na(thf)_2][L^aMoO_2(SPh)]\cdot x$NaX (X = Cl and/or OH; $x \sim 2$). Although it was not incorporated into the product, PPh_4^+ appeared to be essential for the reproducible synthesis of this sodium salt.

The susceptibility of the $[LMoO_2(SPh)]^-$ anions to protonation suggested reactivity toward electrophilic reagents. The anions reacted cleanly with Me_3SiCl, as shown in eq 4.

$$[LMo^VO_2(SPh)]^- + Me_3SiCl \rightarrow LMo^VO(OSiMe_3)(SPh) + Cl^- \quad (4)$$

When ^{18}O-substituted anions were used, the reaction proceeded without loss of label. Bands characteristic of $\nu(Mo^VO)$ and $\nu(SiO)$ modes were observed.

(43) Quantitative analysis of the content of sodium is not available due to the presence of boron and molybdenum in the sample.

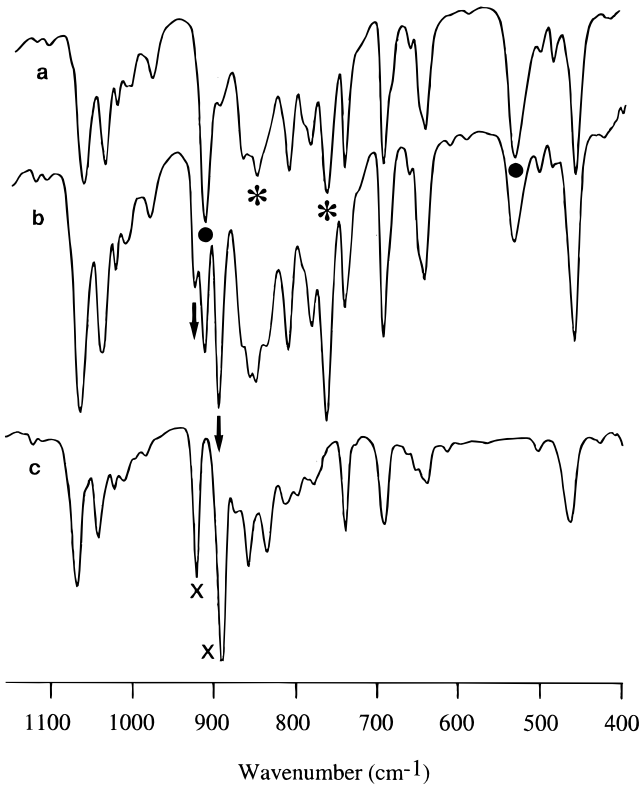

Figure 6. Infrared spectra of the green solid (Nujol mull): (a) initial; (b) after standing in air for 10 min; (c) after standing in air for 30 min. Peaks (*) and (•) are assigned to $[L^aMo^VO_2(SPh)]^-$ and $L^aMo^VO(OH)$-(SPh), respectively. Decomposition of both compounds leads to the in-growth of peaks due to $L^aMo^{VI}O_2(SPh)$ (x).

A Product Containing $L^aMo^VO(OH)(SPh)$. Protonation of $[L^{a,b}Mo^VO_2(SPh)]^-$ to form the conjugate acids $L^{a,b}Mo^VO(OH)$-(SPh) has been demonstrated in dichloromethane (vide supra and ref 23). Attempts to isolate the acid forms from dichloromethane solution were unsuccessful. However, slow evaporation of dichloromethane from a solution of $[CoCp_2][L^aMo^VO_2$-(SPh)] generated in a mixed acetonitrile:dichloromethane solvent system precipitated a green solid containing $L^aMo^VO(OH)(SPh)$. This solid exhibited the electrochemical and EPR properties observed for $[CoCp_2][L^aMo^VO_2(SPh)]$ (Figures 1 and 2). Its infrared spectrum (Figure 6) displayed the strong absorption at 767 cm^{-1} characteristic of $[CoCp_2][L^aMo^VO_2(SPh)]$ and two strong bands at 915 and 535 cm^{-1}, which were absent from the spectrum of $[CoCp_2][L^aMo^VO_2(SPh)]$ (Figure 6a). Upon exposure to air, all three bands were replaced rapidly by the two bands characteristic of $L^aMo^{VI}O_2(SPh)$ (922 and 890 cm^{-1}),[22,23] which can be isolated from the oxidized product. The band at 915 cm^{-1} is typical of a $\nu(Mo^V{=}O)$ mode.[37,44] The band at 535 cm^{-1} is plausibly a $\nu(Mo{-}OH)$ mode. Related L^aMo^VO-(OMe)(SPh)[44] and $LMoO_2(OMe)$[22,23] complexes each exhibit a strong band at *ca.* 540 cm^{-1}, assignable to a $\nu(Mo{-}OMe)$ mode. Transition metal methoxo complexes generally exhibit strong absorptions in the range 300−600 cm^{-1}.[45]

An ^{18}O-labeled sample of the green solid was prepared from $L^aMo^{VI}O_2(SPh)$ (55 atom % ^{18}O content). The infrared spectrum (Figure 7b) clearly revealed the appearance of a new band at 510 cm^{-1}, assignable to the $Mo^V{-}^{18}OH$ isotopomer. Dilution of the label in the product may have resulted from oxygen exchange with the residual water in the solvents during the reaction. The 915 cm^{-1} band appeared to be shifted to *ca.* 840 cm^{-1}, but its clear identification was hampered by interfering bands. The bands assignable to the *cis*-$[Mo^VO_2]^+$ fragment in $[CoCp_2][L^aMo^VO_2(SPh)]$ were also shifted as previously described.

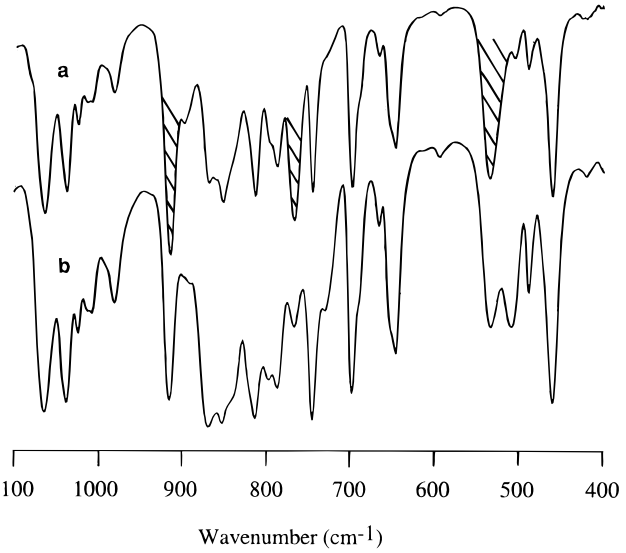

Figure 7. Infrared spectra of the green solid (Nujol mull): (a) 100 atom % ^{16}O; (b) *ca.* 55 atom % ^{18}O. Unobscured bands which shift upon labeling are shaded in (a).

Discussion

The few *cis*-$[Mo^{VI}O_2]^{2+}$ complexes which undergo a reversible, one-electron reduction appear to exhibit two important attributes: (i) minimal ligand conformational change upon reduction, thereby restricting substitution *trans* to the oxo groups, and (ii) the presence of a steric or electrostatic barrier to dimerization of the reduced species.[20,22,23,46] The reversible one-electron chemistry seen for $LMo^{VI}O_2(ER)$ (E = O, S) can be attributed to the facial coordination enforced by L and the combined steric hindrance of L and ER.[23,46] The one-electron reduced *cis*-$[Mo^VO_2]^+$ and *cis*-$[Mo^VO(OH)]^{2+}$ species observed by EPR had never been isolated; in general, they are unstable unless generated under special conditions.[23]

In attempts to isolate *cis*-dioxo-Mo(V) and (hydroxo)oxo-Mo(V) complexes in substance, $LMo^{VI}O_2(SPh)$ complexes were chosen as precursors, since their reduction potentials were more positive and their reduced forms more stable than those of other $LMo^{VI}O_2(ER)$ species.[22,23] A number of reductants were surveyed, but clean products were obtained with cobaltocene only. This reagent provides both the reducing equivalent and the countercation which rapidly precipitates $[CoCp_2][LMo^VO_2$-(SPh)] in these kinetically controlled syntheses. Rapid precipitation of the very unstable compounds is crucial. The dioxygen-scavenging properties of cobaltocene ensure high yields of $[CoCp_2][LMo^VO_2(SPh)]$. Unlike $[L^{a,b}Mo^VO_2(SPh)]^-$, which are protonated readily in solution, $[L^cMo^VO_2(SPh)]^-$ is stable to protonation by adventitious water. This can be attributed to the stronger electron withdrawing properties of the triazolyl rings of L^c relative to the pyrazolyl rings of $L^{a,b}$ and to the presence of the 4-N atoms which may compete with the oxo ligands for protons. These properties permit *slow growth from the reaction*

(44) Xiao, Z.; Bruck, M. A.; Enemark, J. H.; Young, C. G.; Wedd, A. G. Manuscript in preparation.

(45) Adams, R. W.; Martin, R. L.; Winter, G. *Aust. J. Chem.* **1967**, *20*, 773.

(46) Xiao, Z.; Enemark, J. H.; Wedd, A. G.; Young C. G. *Inorg. Chem.* **1994**, *33*, 3438.

mixture[47] of crystals of $[CoCp_2][L^cMo^VO_2(SPh)]$·toluene and the generation of clean EPR spectra. Each of the $[CoCp_2][LMo^{18}O_2(SPh)]$ salts is oxidized quantitatively to $LMo^{VI}O_2(SPh)$ by dioxygen without loss of ^{18}O label. Rapid precipitation of product is a feature of a number of other syntheses of unstable *cis*-dioxo-Ru(VI) and -Os(VI) complexes.[7,12]

Unfortunately, the ready precipitation of the $[CoCp_2][LMo^VO_2(SPh)]$ salts complicates the isolation of the *cis*-$L^{a,b}Mo^VO(OH)(SPh)$ complexes in pure form. A green solid precipitated from a mixed solvent system appears to be a mixture of $L^aMo^VO(OH)(SPh)$ and $[CoCp_2][L^aMo^VO_2(SPh)]$. This interpretation is consistent with the observations that the anion is protonated readily in solution and can be trapped in high yield by the electrophilic reagent Me_3SiCl as the stable complex $L^aMo^VO(OSiMe_3)(SPh)$. These reactions also proceed without loss of ^{18}O label.

Infrared bands due to the ν_s and ν_{as} modes of the *cis*-dioxo-Mo(V) fragment have been assigned on the basis of detailed ^{18}O-labeling studies. The lower energy of the bands relative to those of the Mo(VI) counterparts (Table 4) is consistent with a weakening of the Mo═O bonds upon reduction and single occupation of a π^* MoO_2 molecular orbital. This weakening is also reflected in increased Mo−O distances in the anion compared to its Mo(VI) analogue (vide infra). Significantly, the observation of bands assignable to $\nu_s(MoO_2)$ and $\nu_{as}(MoO_2)$ modes confirms the equivalence of the Mo−O bonds in the $[LMoO_2(SPh)]^-$ complexes. A C_1 $[LMoO(O^{\bullet})(SPh)]^-$ structure having inequivalent Mo−O bonds, which might be envisioned to result from localization of the HOMO along one Mo−O direction, is inconsistent with the infrared data. Such a complex would be expected to exhibit a band typical of the $[Mo^VO]^{3+}$ fragment, in the 900−1000 cm^{-1} region. The MO_2 modes of the following compounds have been assigned as indicated: $ReO_2I(PPh_3)_2$, 923 and 843 cm^{-1};[3] $[ReO_2(bpy)(py)_2]^+$, 904 and 845 cm^{-1} (a band at 767 cm^{-1} was initially[4a] assigned as a potential ReO_2 mode);[4] $[RuO_2(Me_3tcn)(O_2CCF_3)]^+$, 856 and 842 cm^{-1};[8] $[RuO_2(O_2CMe)Cl_2]^-$, 866 and 891 cm^{-1};[7] $[OsO_2(bpy)_2]^{2+}$, 883 and 863 cm^{-1}.[12] None of the above assignments were confirmed by labeling studies. At 870 and 770 cm^{-1}, the $\nu_s(MoO_2)$ and $\nu_{as}(MoO_2)$ modes of the $[LMoO_2(SPh)]^-$ complexes are the lowest in energy yet reported for a *cis*-dioxo species.

The structures of $[CoCp_2][L^cMo^VO_2(SPh)]$ and $L^cMo^{VI}O_2(SPh)$[23] were compared in a brief communication.[29] At 1.742(9) Å, the Mo−O distances in $[L^cMo^VO_2(SPh)]^-$ are slightly longer than the corresponding bonds of $L^cMo^{VI}O_2(SPh)$ (average 1.700(6) Å) and the median distance characteristic of oxo-Mo complexes (1.694 Å).[48] Significantly, the two Mo−O bond distances are equivalent, and there is no unusual thermal behavior associated with the oxo ligands. As well, the O(1)−Mo−O(2) angle of 112.1(4)° in $[L^cMo^VO_2(SPh)]^-$ is increased considerably relative to that of 103.9(2)° in $L^cMo^{VI}O_2(SPh)$. This is associated with an increase in the N(11)−Mo−S angle to 168.9(4)° [cf. 152.7(1)° in $L^cMo^{VI}O_2(SPh)$] and a conspicuous canting of the triazole planes about the Mo···B vector in $[L^cMo^VO_2(SPh)]^-$. The structural features of $L^aMo^{VI}O_2(SPh)$[23] parallel those of $L^cMoO_2(SPh)$ [Mo−O = 1.696(4) Å, O−Mo−O = 102.6(2)°], providing confirmation of shorter Mo−O distances and smaller O−Mo−O angles for the Mo(VI) *vs* Mo(V) compounds. The modest lengthening and equivalence of the Mo−O bond distances in $[L^cMo^VO_2(SPh)]^-$ are consistent with a principally metal-based 3-center π^* HOMO. The increase in the O(1)−Mo−O(2) angle observed for the anion compared to the Mo(VI) analogues is suggestive of repulsion between the d^1 electron and the MoO_2 π-electrons.

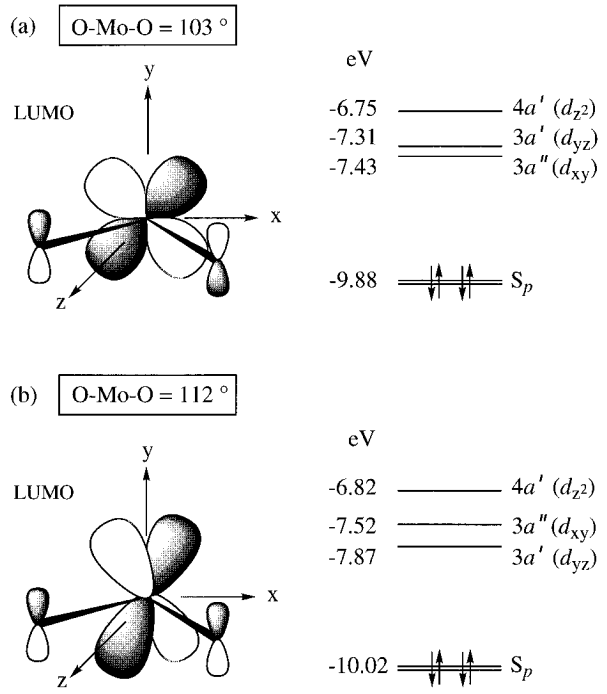

Figure 8. Influence of O−Mo−O angle on frontier orbital energies of $LMo^{VI}O_2(SPh)$ complexes. The LUMO indicated would become the HOMO of a $[LMoO_2(SPh)]^-$ species upon reduction. For the $[LMo^VO_2(SPh)]^-$ complexes, a $3a'(d_{yz})$ HOMO is consistent with the O−Mo−O angle of 112.1(4)° observed for $[L^cMoO_2(SPh)]^-$.[49] Only orbitals within the π-manifold of the MoO_2 unit have been numbered, and only the π^* orbitals are shown in this diagram. Predominant d-orbital contributors to the MOs are indicated in parentheses.

Assuming C_s local symmetry for the $[LMoO_2(SPh)]^{0/-}$ complexes, a π-orbital manifold, comprising three 3-center π-orbitals ($2 \times a' + a''$), their π^* partners ($2 \times a' + a''$), and a nonbonding oxygen p-orbital combination (a''), can be constructed from symmetry-adapted linear combinations of the four oxygen p_π and three molybdenum d_π orbitals. We define the *x* axis as being perpendicular to the mirror plane (*yz*) with the *z* axis bisecting the O−Mo−O angle, as shown in Figure 8. EHMO calculations suggest that the 3a′ and 3a″ MoO_2 π^* orbitals of the $LMo^{VI}O_2(SPh)$ complexes are close in energy and sensitive to changes in the O−Mo−O angle. For $LMo^{VI}O_2(SPh)$, with an O−Mo−O angle of 103°,[23] the d_{xy}-based 3a″ π^* MO is predicted to be the LUMO (Figure 8a). However, if the O−Mo−O angle is increased to 112°, the d_{yz}-based 3a′ orbital becomes the LUMO (Figure 8b). An increase in the O−Mo−O angle increases a″ valence orbital overlap but decreases a′ valence orbital overlap. Consequently, the 3a′ π^* MO is stabilized relative to the 3a″ π^* MO as the O−Mo−O angle increases. Importantly, the orbitals are very close in energy for all the reasonable O−Mo−O angles available to a *cis*-$LMoO_2$ fragment.

Given the limitations of EHMO calculations, either of the $3a'(d_{yz})$ or $3a''(d_{xy})$ MOs could be the HOMO (magnetic orbital) in the $[LMo^VO_2(SPh)]^-$ complexes. Both would be compatible with the observed low-energy $\nu_s(MoO_2)$ and $\nu_{as}(MoO_2)$ modes and the nucleophilic behavior of the anions. However, the

(47) The instability of the complexes is evident in the slow (days) dissolution of freshly precipitated $[CoCp_2][L^aMoO_2(SPh)]$ in its mother liquor, with concomitant formation of crystals of $[CoCp_2]_2[Co(SPh)_4]$. This compound, partially characterized by an X-ray diffraction study (Enemark, J. H.; Bruck, M., private communication) contains a previously reported anion: (a) Holah, D. G.; Coucouvanis, D. *J. Am. Chem. Soc.* **1975**, *97*, 6917. (b) Swenson, D.; Baenziger, N. C.; Coucouvanis, D. *J. Am. Chem. Soc.* **1978**, *100*, 1932.

(48) Orpen, A. G.; Brammer, L.; Allen, F. H.; Kennard, O.; Watson, D. G.; Taylor, R. *J. Chem. Soc., Dalton Trans.* **1989**, S1.

increase in the O(1)−Mo−O(2) angle from 103.9(2)° in L^c-$Mo^{VI}O_2$(SPh) to 112.1(4)° in $[L^cMo^VO_2(SPh)]^-$ favors a 3a′-(d_{yz}) HOMO in the latter (cf. Figure 8b).[49] Assuming this to be the case, the $\boldsymbol{g}$ and $\boldsymbol{A}$(^{95,97}Mo) tensor components can be calculated to first-order in spin−orbit coupling:[50−52]

$$g_{zz} = 2.0023 - \frac{2\alpha^2\epsilon^2\xi}{\Delta E_{xz}}$$

$$g_{xx} = 2.0023 - \frac{2\alpha^2\delta^2\xi}{\Delta E_{x^2-y^2}} - \frac{6\alpha^2\gamma^2\xi}{\Delta E_{z^2}}$$

$$g_{yy} = 2.0023 - \frac{2\alpha^2\beta^2\xi}{\Delta E_{xy}}$$

$$A_{zz} = P\left[-\alpha^2\kappa + (g_{zz} - 2.0023) + \frac{2\alpha^2}{7} + \frac{3\xi}{7}\left\{\frac{\alpha^2\beta^2}{\Delta E_{xy}} - \frac{\alpha^2\gamma^2}{\Delta E_{z^2}} + \frac{\alpha^2\delta^2}{\Delta E_{x^2-y^2}}\right\}\right]$$

$$A_{xx} = P\left[-\alpha^2\kappa + (g_{xx} - 2.0023) - \frac{4\alpha^2}{7} - \frac{3\xi}{7}\left\{\frac{\alpha^2\beta^2}{\Delta E_{xy}} + \frac{\alpha^2\epsilon^2}{\Delta E_{xz}}\right\}\right]$$

$$A_{yy} = P\left[-\alpha^2\kappa + (g_{yy} - 2.0023) + \frac{2\alpha^2}{7} + \frac{3\xi}{7}\left\{\frac{\alpha^2\gamma^2}{\Delta E_{z^2}} - \frac{\alpha^2\delta^2}{\Delta E_{x^2-y^2}} + \frac{\alpha^2\epsilon^2}{\Delta E_{xz}}\right\}\right]$$

where $\Delta E_i = E_i - E_{yz}$, ξ is the spin−orbit coupling constant for Mo^V in the complexes, $P = g_e g_N \beta_e \beta_N \langle r^{-3}\rangle_{4d}$, and κ is the isotropic hyperfine constant in the complexes. As a consequence of the σ^* nature of d_{xz}, which is directed at two oxygen and two nitrogen atoms, ΔE_{xz} will be large and g_{zz} is predicted to be close to the free-electron g value. On the other hand g_{xx} and g_{yy} will be significantly lowered by spin−orbit coupling and the energetic accessibility of the d_{xy} and d_{z^2} orbitals. Thus, we conclude that $g_{zz} > g_{xx}, g_{yy}$. Accordingly, g_{zz} may be confidently assigned to g_1 in Table 3. This assignment is consistent with the observation of ^{35,37}Cl superhyperfine coupling in the g_1 component of $[L^cMo^VO_2Cl]^-$,[23] as overlap of the HOMO and the p_z orbital of Cl (sited on the y axis) provides a mechanism for coupling in this direction. Further, from the equations for A_{ii} above, it is predicted that $|A_{xx}| > |A_{zz}|, |A_{yy}|$. This permits the assignment of g_{xx} as g_3 in Table 3, as this component of $\boldsymbol{g}$ is associated with the largest component of $\boldsymbol{A}$. As well, superhyperfine coupling to ^{17}O is predicted to be strongest in the y direction when the HOMO is the d_{yz} orbital, i.e., the largest ^{17}O superhyperfine component should be associated with $g_2 = g_{yy}$. For $[(L\text{-}N_2S_2)Mo^VO_2]^-$, the only *cis*-dioxo-Mo(V) complex for which ^{17}O coupling data are available, the largest ^{17}O superhyperfine coupling is associated with g_2.[27] Previously, an assignment of the EPR spectrum of $[(L\text{-}N_2S_2)Mo^VO_2]^-$ was made assuming a d_{xy}-based magnetic orbital.[26,27] The possibility of a d_{yz}-based ground state for $[(L\text{-}N_2S_2)Mo^VO_2]^-$ should now be considered,[53] given the bonding implications of the structure of $[L^cMo^VO_2(SPh)]^-$ reported herein. Recent *ab initio* and INDO MO calculations[2h] on $[(L\text{-}N_2S_2)Mo^VO_2]^-$ and $[(L\text{-}N_2O_2)Mo^VO_2]^-$ support a close structural and electronic relationship between $[(L\text{-}N_2S_2)Mo^VO_2]^-$ and the $[LMo^VO_2(SPh)]^-$ complexes reported herein.[54] The isolation and full characterization of the $[CoCp_2][LMo^VO_2(SPh)]$ complexes provides strong confirmation of the essential nature of previously postulated *cis*-dioxo-Mo(V) complexes.[20,21,24−27]

Nucleophilic attack by $[LMo^VO_2(SPh)]^-$ leads (variously) to $LMo^VO(OR)(SPh)$ complexes (R = H, $SiMe_3$, Me). We have presented evidence to support the first isolation of a *cis*-(hydroxo)oxo-Mo(V) complex, $L^aMo^VO(OH)(SPh)$, albeit in a form contaminated by its conjugate base. The *cis* structure is proposed on the basis of the *facial* coordination of L^a and the crystal structures of the related $L^aMo^VO(OSiMe_3)(SCH_2Ph)$ and $L^aMo^VO(OSiMe_3)(NCS)$ complexes.[55] It appears that $[CoCp_2][L^aMo^VO_2(SPh)]$ and $L^aMo^VO(OH)(SPh)$ coprecipitate as a consequence of the equilibrium in eq 2. The EPR spectra of $L^aMo^VO(OH)(SPh)$ are related to those of previously *in situ* generated $[MoO(OH)]^{2+}$ complexes.[23] Protonation and other nucleophilic reactions of the *cis*-$[MoO_2]^+$ moiety may be promoted by the spectator oxo effect described by Rappe and Goddard.[2d,e]

Conclusion

Careful control of the steric and electronic properties of ligands L and X in the $[LMoO_2X]^{0/-}$ species[22,23] has permitted the isolation of a number of *cis*-dioxo-Mo(V) complexes for the first time. Fine-tuning of the basicity of L to favor the $[Mo^VO_2]^+$ fragment relative to its conjugate acid, coupled with a careful choice of X to disfavor condensation, was the key to the isolation of these highly oxygen-sensitive species. One-

(49) The results of the EHMO calculations and the choice of a d_{yz}-based magnetic orbital are supported by near-IR/IR studies of $[L^cMo^VO_2(SPh)]^-$ (which is more stable than the other species and resistant to protonation in solution). Transitions at ca. 2800 and 8500 cm^{-1} are predicted on the basis of the EHMO calculations summarized in Figure 8b. Near-IR/IR spectroelectrochemistry of $[L^cMo^{VI}O_2(SPh)]^{0/-}$ (50 mM, 0.15 M $Bu^n_4NBF_4/CD_2Cl_2$) reveals spectral changes in the 3000 to 3500 cm^{-1} region, which we tentatively ascribe to a band in that region of the spectrum of $[L^cMo^VO_2(SPh)]^-$. A band at 9000 cm^{-1} (1110 nm) is definitely present in the near-IR spectrum of $[CoCp_2][L^cMo^VO_2(SPh)]$ (Experimental Section). The generation of the anion in the spectroelectrochemical experiment was confirmed by the appearance of the near-IR band at 9000 cm^{-1}.

(50) McGarvey, B. R. In *Transition Metal Chemistry*; Carlin, R. L., Ed.; Dekker: New York, 1966; Vol. 3, pp 89−201.

(51) Mabbs, F. E.; Collison, D. *Electron Paramagnetic Resonance of d Transition Metal Compounds*; Elsevier: Amsterdam, 1992.

(52) In the derivation of these equations, the effects of covalent bonding and symmetry allowed d-orbital mixing are ignored, viz., orbitals of the following form are employed (in increasing energy): HOMO = $\phi_1 = \alpha d_{yz} < \phi_2 = \beta d_{xy} < \phi_3 = \gamma d_{z^2} < \phi_4 = \delta d_{x^2-y^2} < \phi_5 = \epsilon d_{xz}$. The possible d orbital mixings in the antibonding orbitals are the following: HOMO = $\phi_1 = \alpha[a_1 d_{yz} + b_1 d_{z^2} + c_1 d_{x^2-y^2}]$, $a_1 > b_1, c_1$; $\phi_2 = \beta[e_2 d_{xy} + f_2 d_{xz}]$, $e_2 > f_2$; $\phi_3 = \gamma[a_3 d_{yz} + b_3 d_{z^2} + c_3 d_{x^2-y^2}]$, $b_3 > a_3, c_3$; $\phi_4 = \delta[a_4 d_{yz} + b_4 d_{z^2} + c_4 d_{x^2-y^2}]$, $c_4 > a_4, b_4$; $\phi_5 = \epsilon[e_5 d_{xy} + f_5 d_{xz}]$, $f_5 > e_5$. Complete expressions for g_{ii} and A_{ii} may be developed using the treatments given in refs 50 and 51 (Chapter 9), but without additional information (e.g., orbital coefficients, assigned spectra, etc.) they provide little further insight into possible assignments.

(53) In the coordinate system adopted, the following predictions are made for an $[(L\text{-}N_2S_2)Mo^VO_2]^-$ complex having a d_{xy}-based magnetic orbital: $g_{xx} > g_{yy} > g_{zz}$ and $|A_{zz}| > |A_{xx}|, |A_{yy}|$.[26] Assuming $[(L\text{-}N_2S_2)Mo^VO_2]^-$ to have a d_{yz}-based magnetic orbital leads to the same predictions made here for the $[LMo^VO_2X]^-$ complexes. Definitive assignments in both systems require single crystal data for the $[Mo^VO_2]^+$ species doped into a suitable diamagnetic lattice.

(54) Recent MO calculations on related $[(L\text{-}N_2S_2)MoO_2]^-$ and $[(L\text{-}N_2O_2)MoO_2]^-$ complexes suggest that the electronic structures of dioxo-Mo(V) complexes are also critically dependent on the nature of the coligands.[2h,36] For the N_2S_2-donor complex a metal(4d/5p)-based HOMO (magnetic orbital), a Mo−O distance of 1.69 Å, and a O−Mo−O angle of 109° are predicted. The Mo−O distance is essentially identical to that calculated for the Mo(VI) analogue $(L\text{-}N_2S_2)MoO_2$ but the O−Mo−O angle is considerably larger in the Mo(V) complex. The N_2O_2-donor complex $[(L\text{-}N_2O_2)MoO_2]^-$ is predicted to have a HOMO with significant oxygen p-orbital character, two distinctly different Mo−O distances (1.68 and 1.87 Å) and an O−Mo−O angle of 103°. The structural parameters in this case are distinctly different from those of the analogous Mo(VI) complex.

(55) Bruck, M.; Enemark, J. H. Unpublished results.

electron reduction of $L^cMo^{VI}O_2(SPh)$ results in a lengthening of the Mo−O bond lengths and an opening of the O−Mo−O bond angle, but the two oxo ligands remain equivalent. Correspondingly, the $\nu_s(MoO_2)$ and $\nu_{as}(MoO_2)$ modes of the $[LMo^VO_2X]^-$ complexes are significantly lowered in energy. One of the oxo ligands in the anions may be protonated or silylated due to their increased basicity. The acid $L^aMo^VO(OH)(SPh)$ was also isolated for the first time as a coprecipitate with $[CoCp_2][L^aMo^VO_2(SPh)]$. EPR studies of various pterin-containing molybdoenzymes indicate that (hydroxo)oxo-Mo(V) centers are generated upon enzyme reduction.[27,32,33] However, an EPR signal indicative of a dioxo-Mo(V) center has not been reported for any enzyme. Our results demonstrate that the basicity of the $[Mo^VO_2]^+$ center may be electronically fine-tuned by the coligands. The molybdenum centers in enzymes, it seems, possess coligands which impart high basicity to any nascent $[Mo^VO_2]^+$ center and promote its rapid protonation. This is, of course, a key to the proposed coupled electron−proton transfer steps which appear to regenerate enzyme active sites following oxygen atom transfer between water and substrate.[15,16]

Acknowledgment. We thank Prof. A. Nakamura for providing access to the CAChe workstation on which EHMO calculations were performed, the Japan Society for the Promotion of Science for a fellowship enabling C.G.Y. to visit Japan, Dr. Stephen P. Best for spectroelectrochemical experiments, and Prof. John H. Enemark for helpful discussions. We gratefully acknowledge the financial support of the Australian Research Council.

Appendix

cis-$[Mo^{VI}O_2]^{2+}$ complexes typically exhibit $\nu_s(MoO_2)$ and $\nu_{as}(MoO_2)$ modes separated by about 30 cm^{-1} in the range 870−950 cm^{-1} with ν_s at higher energy.[56,57] The frequencies of modes ν_{as} and ν_{as}' of nonlinear harmonic oscillators YXY and isotopomer Y′XY′ are approximated by eq A1:

$$\left(\frac{\nu_{as}'}{\nu_{as}}\right)^2 = \frac{m_y(m_x + 2m_y' \sin^2\theta)}{m_y'(m_x + 2m_y \sin^2\theta)} \qquad \text{(A1)}$$

where m_x, m_y, and m_y' are atomic masses and θ is half the YXY angle.[58,59] Assuming that *cis*-$[MoO_2]^{2+}$ fragments are independent harmonic oscillators in their complexes, then ν_{as}' for the *cis*-$[Mo^{18}O_2]^{2+}$ center can be estimated from assigned ν_{as} values in *cis*-$[Mo^{16}O_2]^{2+}$ complexes. Results calculated in the present work for $L^{a,b}Mo^{VI}O_2(SPh)$[22,23] and $(L\text{-}NS_2)Mo^{VI}O_2$[60] are consistent with the assignments (Table 4).

Assuming the O−Mo−O bond angle of 112.4° observed in $[CoCp_2][L^cMo^VO_2(SPh)]$ applies to the L^a and L^b salts, estimation of $\nu_{as}(Mo^{18}O_2)$ in $[L^aMo^VO_2(SPh)]^-$ using eq A1 is in excellent agreement with the assignments (Table 4). An equivalent calculation for $[L^bMo^VO_2(SPh)]^-$ predicts $\nu_{as}(Mo^{18}O_2)$ to be close to the approximate value estimated after allowing for overlap with other absorptions (Table 4; Figure 4b).

Similar assumptions to those used to derive eq A1 lead to eq A2:

$$\left(\frac{\nu_s'\nu_\delta'}{\nu_s\nu_\delta}\right)^2 = \frac{m_y^2(m_x + 2m_y')}{m_y'^2(m_x + 2m_y)} \qquad \text{(A2)}$$

where ν_s and ν_δ are YXY symmetric stretching and deformation modes, respectively.[58,59] It follows that, for any two symmetrically labeled YXY fragments A and B, eq A3 holds:

$$\left(\frac{\nu_s'}{\nu_s}\right)_A\left(\frac{\nu_\delta'}{\nu_\delta}\right)_A = \left(\frac{\nu_s'}{\nu_s}\right)_B\left(\frac{\nu_\delta'}{\nu_\delta}\right)_B \qquad \text{(A3)}$$

Assuming $(\nu_\delta'/\nu_\delta)_A = (\nu_\delta'/\nu_\delta)_B$, then $(\nu_s'/\nu_s)_A = (\nu_s'/\nu_s)_B$. This appears to be true for *cis*-$[Mo^{VI}O_2]^{2+}$ centers: for the nine *cis*-$[Mo^{VI}O_2]^{2+}$ complexes reported in Table 4 and references 61 and 62, $(\nu_s^{18}/\nu_s^{16}) = 0.950 \pm 0.001$. Absorptions assignable to $\nu_s(Mo^{18}O_2)$ are clearly seen in the spectra of $[CoCp_2][L^{a,b}\text{-}Mo^VO_2(SPh)]$ (Table 4, Figure 4) at 822 and 835 cm^{-1}, respectively. Application of the above ratio, derived for Mo^{VI}, to these Mo^V species predicts $\nu_s(Mo^{16}O_2)$ values close to those assigned tentatively (Table 4).

Supporting Information Available: Tables of crystal data, final atomic coordinates, anisotropic temperature factors, and bond lengths and angles (10 pages) for $[CoCp_2][L^cMoO_2(SPh)]\cdot$-toluene. This material is contained in many libraries on microfiche, immediately follows this article in the microfilm version of the journal, can be ordered from the ACS, and can be downloaded from the Internet; see any current masthead page for ordering information and Internet access instructions.

JA952525A

(56) Griffith, W. P.; Wickins, T. D. *J. Chem. Soc. A* **1968**, 400.
(57) Griffith, W. P. *J. Chem. Soc. A* **1969**, 211.
(58) Herzberg, G. *Infrared and Raman Spectra of Polyatomic Molecules*; D. Van Nostrand: Princeton, NJ, 1945; p 228 and 231.
(59) Pinchas, S.; Laulicht, I. *Infrared Spectra of Labelled Compounds*; Academic: New York, 1971; pp 27−28.
(60) Craig, J. A.; Holm, R. H. *J. Am. Chem. Soc.* **1989**, *111*, 2111.
(61) (a) Newton, W. E.; McDonald, J. W. *Proceedings of the Second International Conference on the Chemistry and Uses of Molybdenum*; Mitchell, P. C. H., Seaman, A., Eds.; Climax Molybdenum Company: Michigan, 1976; pp 25−30. (b) Newton, W. E.; McDonald, J. W. *J. Less-Common Met.* **1977**, *54*, 51.
(62) Corbin, J. L.; Miller, K. F.; Pariyadath, N.; Wherland, S.; Bruce, A. F.; Stiefel, E. I. *Inorg. Chim. Acta* **1984**, *90*, 41.